Fourier transform infrared spectroscopy provides an evidence of papain denaturation and aggregation during cold storage

Brankica Rašković, Milica Popović, Sanja Ostojić, Boban Anđelković, Vele Tešević, Natalija Polović

PII: S1386-1425(15)00674-5
DOI: http://dx.doi.org/10.1016/j.saa.2015.05.061
Reference: SAA 13729

To appear in: *Spectrochimica Acta Part A: Molecular and Biomolecular Spectroscopy*

Received Date: 12 January 2015
Revised Date: 6 May 2015
Accepted Date: 12 May 2015

Please cite this article as: B. Rašković, M. Popović, S. Ostojić, B. Anđelković, V. Tešević, N. Polović, Fourier transform infrared spectroscopy provides an evidence of papain denaturation and aggregation during cold storage, *Spectrochimica Acta Part A: Molecular and Biomolecular Spectroscopy* (2015), doi: http://dx.doi.org/10.1016/j.saa.2015.05.061

Fourier transform infrared spectroscopy provides an evidence of papain denaturation and aggregation during cold storage

Brankica Rašković[1], Milica Popović[1], Sanja Ostojić[2] Boban Anđelković[3], Vele Tešević[3] and Natalija Polović[1]*

[1]Department of Biochemistry, University of Belgrade – Faculty of Chemistry, Studentski trg 12 – 16, 11000 Belgrade, Republic of Serbia

[2]Institute of General and Physical Chemistry, Studentski trg 12, 11000 Belgrade, Republic of Serbia

[3]Department of Organic chemistry, University of Belgrade – Faculty of Chemistry, Studentski trg 12 – 16, 11000 Belgrade, Republic of Serbia

*Correspondence:

Natalija Polović, PhD

University of Belgrade – Faculty of Chemistry, Department of Biochemistry, Studentski trg 12 – 16, 11000 Belgrade, Republic of Serbia, Phone: +381113336721, Fax: +381112184330, E-mail: polovicn@chem.bg.ac.rs

Abstract

Papain is a cysteine protease with wide substrate specificity and many applications. Despite its widespread applications, cold stability of papain has never been studied. Here, we used differential spectroscopy to monitor thermal denaturation process. Papain was the most stabile from 45ºC to 60ºC with ΔG^{o}_{321} of 13.9 ± 0.3 kJ/mol and Tm value of 84 ± 1ºC. After cold storage, papain lost parts of its native secondary structures elements which gave an increase of 40% of intermolecular β-sheet content (band maximum detected at frequency of 1621 cm^{-1} in Fourier transform infrared (FT-IR) spectrum) indicating the presence of secondary structures necessary for aggregation. The presence of protein aggregates after cold storage was also proven by analytical size exclusion chromatography. After six freeze-thaw cycles around 75% of starting enzyme activity of papain was lost due to cold denaturation and aggregation of unfolded protein. Autoproteolysis of papain did not cause significant loss of the protein activity. Upon the cold storage, papain underwent structural rearrangements and aggregation that correspond to other cold denatured proteins, rather than autoproteolysis which could have the commercial importance for the growing polypeptide based industry.

Keywords: papain, FT-IR, cold stability, cold denaturation, cold inactivation, aggregation

1. Introduction

Papain is a cysteine protease (EC 3.4.22.2) with wide substrate specificity and many applications. It has been isolated from the latex of the papaya fruit. The preprotein consists of 345 amino acids and it is secreted as zymogene [1]. After the cleavage of the activation peptide, the mature enzyme contains 212 amino acid residues organized in two domains. The N-terminal domain has mainly α-helical structure while C-terminal domain has antiparallel β-sheet fold [2]. Papain is extensively used as meat tenderizer [3], in dental caries removal procedures [4], for preparation of clinically relevant antibody fragments [5], as a cell dissociation/debris removal agent [6], as a component in cosmetics [7] and detergents [8]. The main limitation in usage of proteolytic enzymes in many applications is their temperature stability, both at elevated temperatures and during freezing. It has been already shown that papain is stable at elevated temperatures with Tm value at 83 ± 1°C [9]. However, cold stability (especially after freezing and thawing) of papain has never been studied.

During freezing and storage of proteins in frozen state, several factors can impact protein stability. Cold denaturation of globular proteins has been detected in several cases especially at high pressure [10-13]. Theoretically, cold denaturation should happen as a consequence of changes in interactions between water and protein molecules at low temperatures thus should represent a universal phenomenon. However, cold denaturation is difficult to study since most proteins have denaturation points below 0ºC [14]. Further, the denaturation of a protein during freezing could also occur as a consequence of changes in solute concentration due to ice formation and changes of pH value in the protein surrounding [15]. Freeze-thaw cycles are

routinely used as a tool to determine the combined effects of these different freezing related stresses on protein stability [15, 16].

The aim of this paper was to study cold storage stability of papain. We describe a significant loss of papain activity as a consequence of cold storage. This phenomenon could be of importance for industrial conservation of the enzyme since cold storage of papain leads to its denaturation and aggregation.

2. Materials and methods

2.1 Papain purification

In order to remove inactive/denatured protein and low molecular weight compounds, papain was purified from commercial papain preparation (The British Drug House Ltd, London, England). Papain was extracted from dry powder with 100 mM Tris buffer pH 8 containing 100 mM NaCl and 1 mM ethylenediaminetetraacetic acid disodium salt (EDTA) for 30 minutes at 10°C. Extract was centrifuged for 15 minutes at 4000 x g at 10 °C and obtained supernatant was further used. Papain was precipitated from supernatant by addition of 2 volumes of ice cold acetone followed by incubation at -20ºC for 30 minutes. The precipitate was separated by centrifugation at 10 000 x g for 5 minutes at 4ºC, dried and resuspended in 100 mM Tris buffer pH 8 containing 100 mM NaCl and 1 mM EDTA for further purification. Covalent chromatography was performed on Thiol-Sepharose 4B (GE Healthcare, Uppsala, Sweden). Matrix was equilibrated in 100 mM Tris buffer pH 8.0 containing 100 mM NaCl and 1 mM EDTA (20 column volumes (CV)) first, then the sample was applied. Unbound proteins were eluted with 20 CV of 100 mM Tris buffer pH 8 containing 100 mM NaCl and 1 mM EDTA, while bound protein was eluted by addition of 10

mM L-cysteine to the starting buffer. The homogeneity of purified protein was analyzed by sodium dodecyl sulfate polyacrylamide gel electrophoresis (SDS-PAGE). The activity was analyzed by zymography and Nα-Benzoyl-L-arginine 4-nitroanilide hydrochloride (BAPNA) hydrolysis. Concentration of the purified protein was determined using Bradford method. Bovine serum albumin (BSA) was used as standard [17].

2.2 SDS PAGE and zymogram

For in gel analysis of proteolytic activity detection papain was resolved under reducing conditions in a discontinuous buffer system SDS-PAGE with a 4% stacking gel and 12% resolving gel in a Hoefer Dual Gel Mighty Small SE 245 vertical electrophoresis system (Hoefer, Holliston, USA) according to Laemmli [18]. The amount of 2.5 µg/mm of the protein was applied on the gel. To detect proteolytic activity of papain after SDS–PAGE, zymograms were developed according to Felicioli et al. [19] with some modifications. Briefly, after incubation in non reducing sample buffer (1 h at 60°C and 5 minutes at 95°C), protein samples were applied onto a 12% resolving gel co-polymerized with 0.1% gelatin for SDS–PAGE analysis. After electrophoresis, the gel was incubated in a 100 mM Tris, pH 8 with 100 mM NaCl 1 and mM EDTA for 16 h, followed by staining with Coomassie Brilliant Blue R-250 (CBB) (Serva, Heidelberg, Germany).

2.3 Trypsin mass fingerprinting

Protein spot was excised from CBB stained gel to perform in-gel trypsin digestion according to the manufacturer instructions. Obtained peptides were injected onto a reversed phase C18 column (ACQUITY UPLC BEH 130, 1.7 µm, 2.1 x 50 mm, Waters, Milford, MA, USA)

installed on Acquity ultra-performance liquid chromatography (UPLC) system (Waters, Milford, MA, USA) and separated using acetonitrile gradient (0-50% for 40 min with 0.1% formic acid). After detection with photodiode array (UV) at 280 nm mass spectra were recorded on triple-quadrupole mass spectrometer (ACQUITY TQD, Waters, Milford, MA, USA) in positive ion mode with capillary voltage of 3 kV and drying gas flow rate of 8.3 L/min at 250ºC. The scan range was set from 400 to 2000 m/z. The peptide masses were searched against the SwissProt protein sequence database using the MASCOT program.

2.4 Differential UV Spectroscopy

UV absorbance measurements were performed on Evolution 300 spectrophotometer (Thermo Fisher Scientific, Madison, USA) using matched 1 cm path length quartz cuvettes. The spectrophotometer was equipped with an electrothermal temperature controller which provides thermal programmability for the multiple cell units so that the absorbance measurements can be performed directly as a function of temperature. Spectra of native (room temperature) or thermally denatured papain (99°C) were recorded from 230 nm to 300 nm in 50 mM Tris buffer pH 8.0. Papain concentration was 1 mg/mL. Spectra of buffer only served as a blank. Equilibrium thermal unfolding of papain was monitored by recording absorbance at 230, 267 and 286 nm as a function of temperature over the appropriate temperature range (5-99°C). The UV difference spectrum was calculated by subtraction of absorbances of fully native and fully denatured papain at all wavelengths in the recorded region as described by Hatley and Franks [20]. The wavelength 267 nm was chosen for further analysis as the maximal difference between the denatured and the native protein spectra was observed at this wavelength. The heating rate was 0.5°C min^{-1}.

Using UV spectroscopy we were able to calculate Gibbs free energy (ΔG^{o}) of papain denaturation at different temperatures. Fraction of thermally denatured papain (F_d) was calculated using equation:

$$F_d=(Y_N-Y_{obs})\times(Y_N-Y_D)^{-1} \quad [1]$$

In the given equation Y_{obs} represents the observed value of absorbance, while Y_N and Y_D represents absorbance values characteristic of fully native and fully denatured papain, respectively.

From the following equation, equilibrium constant of the process (K) could be obtained:

$$K=F_d(1-F_d)^{-1} \quad [2]$$

Calculated values for F_d and K were further used for Gibbs free energy calculation according to the following equation:

$$\Delta G^{o}=-RT\ln K \quad (3)$$

Where R is universal gas constant and T is the absolute temperature [21].

2.5. Differential scanning calorimetry (DSC)

All thermograms were acquired on a DSC Q1000 series (TA Instruments, New Castle, Delaware) with an auto sampler and a refrigerated cooling system (RCS, TA Instruments). Approximately 7 mg of the protein solution (10 mg/ml) in 50 mM Tris buffer pH 8.0 was weighed into an aluminum pan and hermetically sealed with an aluminum cover. Reference pan was filled with adequate weight of buffer solution. Sample was equilibrated on 10°C and then heated to 90°C at a heating rate of 1°C/min. Temperature maximum (Tm) of the endothermal transition corresponding to protein denaturation was determined by TA Instruments Universal Analysis 2000 software (version 4.1D).

2.6 Papain activity measurement

Biological activity of purified papain was tested using BAPNA (Sigma-Aldrich, Steinheim, Germany) as a substrate in a 96-well microtitre plate (Sarstedt, Numbrecht, Germany) as described in Raskovic et al. [22] with some modifications. Briefly, 100 µL substrate solution (1mM BAPNA in 100 mM Tris buffer pH 8.0 with 1 mM EDTA and 10 mM L-cysteine) was mixed with aqueous papain solution (25 µL) incubated at 25°C. After 60 min the reaction was stopped by the addition of glacial acetic acid and the absorbance at 405 nm was measured.

2.7 Freeze-thaw cycles

One hundred microliters of purified papain was frozen at -20°C in 1.5 mL centrifuge tubes. After one hour the samples were thawed at the room temperature. Freeze-thaw cycles were repeated up to six times. Relative activity of papain was determined after each cycle as activity remaining in the sample. Starting activity detected in the sample was considered as 100%. All experiments were repeated three times.

2.8 Autoproteolysis measurement

Autoproteolysis was measured as described previously [23] with some modifications. To test the autoproteolysis 10 µL of 0.2 mg/mL papain solution was used. An aliquot was immediately tested for autoproteolysis. Solutions were subjected to 6 freeze-thaw cycles as already described. After each cycle, an aliquot (10 µL) was mixed with 200 µL of CBB (0.125% Coomassie Brilliant Blue G-250 in 24% ethanol and 48% phosphoric acid). After 5 minutes, the absorbance at 620 nm was measured. The assay was performed in triplicate.

2.9 Reverse-phase chromatography analysis of autoproteolytic products

Reverse-phase chromatography of the untreated papain and freeze-thawed papain samples at concentration 1 mg/mL was performed using an Äkta Purifier 10 System (GE Healthcare, Uppsala, Sweden) on a Discovery® BIO Wide Pore C5-5 10 cm × 4.6 mm, 5µm (Supelco, Bellefonte, PA, USA) column. The protein was eluted using an acetonitrile gradient (0-90% for 10 column volumes with 0.1% trifluoroacetic acid).

2.10 Secondary structures determination - Fourier transform infrared spectroscopy

Infrared spectra were recorded for all: native, thermally treated (5 minutes at 95°C) and cold stored papain (freeze-thawed for 6 times) using Fourier transform infrared spectroscopy (FT-IR) with an attenuated total reflectance (ATR) at 1 cm^{-1} resolution (Nicolet 6700 FT-IR, software OMNIC, Version 7.0, Thermo Scientific, USA). Concentration of the solution of papain samples was 10 mg/mL. Ten microliters of these solutions were applied onto a Smart accessory with diamond crystal (Smart Orbit, Thermo Scientific, USA). Solvent was evaporated by the nitrogen stream in order to obtain thin ATR film. For each spectrum, 64 scans were collected. The spectrum of the buffer was subtracted from the spectrum of protein since it is known to interfere with the protein absorbance in the amide I region. After subtraction, spectrum was smoothed in order to remove the noise (factor of 6.75 cm^{-1}). Criteria for the correctness of subtraction were removal of the band near 2200 cm^{-1}. The region between 1700 cm^{-1} and 1600 cm^{-1} (the amide I region) was fitted. The procedure of curve-fitting was used to decompose the original amide I spectra to its Gaussian–Lorentzian curve constituents that would be assigned to certain structural features. The contribution of each curve to the amide I band was assessed by integrating the area under the curve, and then normalizing it to the total area under the amide I band.

Assignment of secondary structures for all the observed peaks was done according to previously published guidelines [24-27].

2.11 Monitoring of aggregation and estimation of molecular weight of papain by size exclusion chromatography

Analytical size exclusion chromatography was performed using Äkta Purifier 10 System (GE Healthcare, Uppsala, Sweden) on Superdex 75 PC 3.2/30 column. Column was equilibrated with 100 mM Tris buffer pH 8 containing 100 mM NaCl and 1 mM EDTA. Papain solution (10 µL, concentration 1 mg/ml) was applied to the column at flow rate 0.05 µL/min. The calibration of the column was performed using the mixture of gel filtration molecular weight standards (1 mg/mL each): bovine serum albumin (67 kDa), carbonic anhydrase (29 kDa), cytochrome c (14 kDa) and aprotinin (6.5 kDa) (Sigma-Aldrich, Steinheim, Germany). To determine void volume, blue dextran (Sigma-Aldrich, Steinheim, Germany) was used.

Elution volume of molecular weight standards was used to create calibration chart (Ve/Vt= f (log Mw)). Molecular weight of papain was estimated from the calibration chart.

3. Results

3.1 Papain purification

Due to interference of low molecular weight contaminants in spectroscopic methods [28], we first sought to purify papain. Acetone precipitation and covalent chromatography were used for the purification of papain from commercial preparation. Protein concentration was determined using Bradford method, while activity was monitored with BAPNA as a substrate. Acetone

precipitation did not cause loss of activity since specific activity remained the same (1.2 U/mg) as in crude papain extract (Table 1).

However, pigments and low molecular weight contaminants were removed rendering the papain solution colorless. Covalent chromatography enabled further purification of the protein, 7.9 times when compared to the starting sample (Table 1, Fig. 1A).

Purification and activity was also monitored by SDS-PAGE and zymogram (Fig. 1B). Samples incubated at 60°C retained activity while it was lost in the samples incubated at 95°C. Slower migration of papain was visible in all the bands incubated at 60°C in comparison to those incubated at 95°C.

3.2 Papain identification by TMF

After SDS-PAGE and CBB staining of protein isolated by acetone precipitation and covalent chromatography, we identified the isolated protein by proteomic analysis after trypsin digestion. According to Mascot, protein scores greater than 70 were considered as significant ($p<0.05$). Papain was identified by 12 matching peptides, with sequence coverage of 27%, as the only significant hit (Mascot score was 116) (Fig. 1C).

3.3 Thermal denaturation of papain

In UV absorption spectra from 255 nm to 300 nm (Fig. 2A) a clear difference between native and denatured molecule of papain was observed. Absorption extinction coefficient (ε) maximum of native molecule was at 279 nm ($58.332 cm^{-1}mM^{-1}$), while it was shifted toward shorter wavelengths for the denatured molecule (275nm, $63.855\ cm^{-1}mM^{-1}$).

For observing differences in UV spectra between native and denatured molecule a differential UV spectra was calculated (Fig. 2B) as described by Hatley and Franks [20]. The greatest difference in the extinction coefficient was observed at 267 nm and it was $\Delta\varepsilon$ = -8.912 $cm^{-1}mM^{-1}$. This wavelength was used for monitoring papain denaturation in further experiments.

In order to examine thermal denaturation curve of papain, absorbance at 267 nm was observed in temperature range from 5-99ºC. Papain was incubated at given temperature for 2 minutes before the measurement was performed. Percentage of native structure was expressed in relation to A_{267} at 57ºC (Fig. 2C). Papain is the most stabile from 45ºC to 60ºC, with the maximum at 57ºC, as observed from the denaturation curve. From 60ºC to 95ºC percent of native structure is reduced from 99.5% to only 0.5%. In a part of the curve below 45ºC reduction in percent of native structure can be noted as well, and at 5ºC, 15% reduction was observed.

Thermal denaturation Tm value is determined to be 84 ± 1ºC. The same value was determined by differential scanning calorimetry (Supplementary Fig. 1).

Thermodynamics parameter (ΔG^o) of papain denaturation process was calculated for 5ºC, 25ºC, 48ºC and 60ºC as described in Yousefi et al. [21]. Results are presented in Table 2.

3.4 Cold storage stability of papain

Activity of papain after cold storage at -20ºC was observed using BAPNA as a substrate (Fig. 3). Residual activity was determined after each of 6 freeze and thaw cycles. After 6^{th} cycle about 75% of activity was lost.

3.5 Papain autoproteolysis

Papain autoproteolysis during 6 freeze-thaw cycles was monitored using an assay based on CBB binding (Fig. 4A) and to estimate the damage to papain, reverse phase high performance liquid chromatography (RP-HPLC) was performed (Fig. 4B).

We did not detect significant autoproteolysis of papain both in the CBB-binding based assay and in RP-HPLC.

3.6 Secondary structure determination

Infrared data were obtained for all: native, thermally treated and cold stored papain. The changes in the Savitzki-Golay second derivative spectra (amide I region) are presented in Fig. 5.

In the second derivative spectrum of native papain several important bands could be observed, especially in the region that could be attributed to most important ordered secondary structures with the maxima at frequencies 1630, 1641, 1648, 1659, 1671, 1673, 1683 and 1697 cm^{-1} (Fig. 5A). The most prominent change in the second derivative spectrum of thermally treated papain (Fig. 5B) is the disappearance of 1648 cm^{-1} band that could be attributed to α-helix [24]. The second derivative spectrum of cold stored papain differed from native papain spectrum since the most prominent maximum is shifted to 1621 cm^{-1} indicating the presence of intermolecular β-sheet (Fig. 5C) [26, 27].

After decomposition of amide I region of the FT-IR spectra (Fig. 6), peaks were assigned to specific secondary structures (Table 3), and the relative percentage of each secondary structure was calculated using the contribution of integrated intensities of bands (areas) to the total amide I band area. The content of secondary structures in X-ray determined tertiary structure of papain was calculated from UniProt data bank entry (P00784 (PAPA1_CARPA)). The results are presented in Table 4.

The weak 1610-1614 cm^{-1} band contribution in native state and thermally denatured protein that arises from side-chain vibration [26] was not included in secondary structure estimation. It had also been substracted form the overlapping band at 1618-1623 cm^{-1}.

Goormaghtigh et al. assigned frequencies 1660-1670 cm^{-1} in native papain spectrum to turn structures [24]. Hovewer, the study of Vedantham et al. [25] showed that bands at frequencies 1665-1676 cm^{-1} correspond to unordered helix. In this work, assignment of 1672 cm^{-1} band to unordered helix (Table 3) rather to the turn structure provides better concurrence of estimated secondary structure content of the native papain to the content calculated from X-ray data (Table 4) then the one presented before [24].

Thermal denaturation of papain led to increase in content of β-sheet structures and to decrease of α-helix and unordered structures. Nevertheless, the most pronounced changes in native-like content of secondary structures are induced by papain cold storage (Table 4).

3.7 Aggregation of papain during cold storage

Aggregation of cold stored papain was monitored by size exclusion chromatography. The chromatogram of native papain reveals one major peak of molecular weight 24.0 kDa. In the chromatogram of cold stored protein, peak representing native papain was smaller, while the majority of protein present in the sample eluted in the void volume of the column (Fig. 7).

4. Discussion

To investigate papain stability after cold storage, we first purified commercial papain in order to remove inactive protease and low molecular weight substances that could interfere with

spectroscopic methods. Differential spectroscopy (Fig. 2C, Table 2) and SDS-PAGE zymography (Fig. 1B) showed that papain was stable at elevated temperatures (up to 60ºC). Shift in SDS-PAGE mobility of the native (and active) papain in comparison to denatured one could be explained as a consequence of papain resistance to SDS denaturation. Since, SDS binding to the native molecule of papain was decreased, papain was not completely denatured and its net negative charge was decreased, so shift in SDS-PAGE mobility was very pronounced when compared to completely denatured protein [29]. At 95ºC, high temperature contributes to the denaturation of papain so the protein become completely linearized and fully covered with SDS, which affected its electrophoretic mobility. In addition, molecular weight of the native enzyme determined by size exclusion chromatography confirmed that papain was in a form of monomer, excluding possible oligomerization under native conditions (Fig. 7).

In UV region from 230 nm to 300 nm aromatic amino acids are absorbing and their extinction coefficients are largely dependent upon their mobility and their environments. This is affected by the conformation of the protein, and in native molecule aromatic amino acid residues are usually placed inside hydrophobic core of the protein. During denaturation their extinction coefficient changes consequently affecting the spectra of the entire protein. Differential UV spectrometry has been extensively used in studying protein denaturation [30-32].

The overall problem in monitoring of cold denaturation of proteins is present due to ice formation at low temperatures which interfere with standard methods used for monitoring protein denaturation [14]. However, we were able to capture the beginning of cold denaturation process using differential spectroscopy. The validity of this approach was proven by Tm value determined for the papain denaturation at elevated temperatures, which is comparable to the previously published one (Fig. 2C). Sathish et al. has recently reported Tm value of 83 ± 1ºC for

papain determined by differential scanning calorimetry [9], which is in good agreement with the value that we determined by both methods. In this part of the denaturation curve cooperative denaturation mechanism can be clearly observed. Cold denaturation could also be monitored by measuring A_{230} (data not shown) as recently described [32]. However, we were unable to capture cold transition point using differential scanning calorimetry (Suppl. Fig. 1).

Renaturation curves were also recorded but no significant change in the extinction coefficient was detected, so we concluded that thermal denaturation process is irreversible (data not shown). It is well known that papain family of proteases are secreted as zymogens, thus the cleavage of the activation peptide could affect papain renaturation [2] especially as propeptide can play a role of intramolecular chaperonin ensuring the correct folding of the molecule [33].

FT-IR spectroscopy is well established method for the analysis of protein secondary structure. The mostly used spectral region for secondary structure analysis is amide I band (frequency limits: 1600 – 1700 cm^{-1}), which is due almost entirely to the C=O stretch vibrations of the peptide bonds [34]. Recent studies showed that specific low frequency bands present in the amide I region of FT-IR second derivate spectrum appear when analysed proteins tend to aggregate. Several authors reported that frequencies 1614 - 1624 cm^{-1} and above 1684 cm^{-1} are aggregation specific frequencies, and they appear due to the formation of intermolecular antiparallel β-sheets prior to aggregation [26, 27, 35]. Two peaks at the frequency as low as 1621 cm^{-1} and as high as 1695-1698 cm^{-1} that could be observed in the spectrum of thermally treated and cold stored papain (Fig. 6B and Fig. 6C, respectively) we assigned to aggregation specific intermolecular antiparallel β-sheet. However, we detected similar bands in the spectrum of native papain as well, but their contribution was in total 6.2% in comparison to 21.3% and 46.2% of the total amide I area found in the case of thermally treated and cold stored papain, respectively

(Table 4). The presence of papain aggregates formed upon cold storage was confirmed by analytical size exclusion chromatography (Fig. 7). Just a minor portion of native papain could be detected in the chromatogram of cold stored protein explaining such a dramatic activity loss after six freeze-thaw cycles (Fig. 3). Monitoring of papain autoproteolysis by CBB binding and RP-HPLC (Fig. 4) suggests that detected inactivation of 75% (Fig.3) cannot be attributed to papain autoproteolysis.

A theory behind denaturation of proteins in the frozen state claims destabilization of protein native structure since hydrophobic interactions become weaker with decreasing temperature which leads to the exposure of non-polar residues to water accounting for unfolding [36]. Several authors had reported the increase of β-sheet content in cold denatured proteins compared to the native ones [37, 38]. Furthermore, computer simulations have shown that this could be related to formation of a thin layer of water around non-polar residues that is favourable at low temperatures. This thin layer can be accommodated between residues that form β-sheet structures but not α-helix [39, 40]. Since cold denatured states tend to favour the formation of β-sheets which are building blocks of fibril-like aggregates [41] it could be of importance for protein activity loss during thawing or lyophilisation.

Denaturation and aggregation of proteins during cold storage, especially the ones with commercial application is of particular concern to ever growing polypeptide based industry [42]. Despite of general belief that the activity loss detected upon the cold storage of proteases happens as a consequence of autoproteolysis, in this work it is undoubtedly shown that upon the cold storage papain underwent structural rearrangements and aggregation that correspond to other cold denatured proteins, rather than autoproteolysis.

Studying cold stability of industrially important proteases, including papain, could lead to development of better preservation methods (the usage of cryoprotectants) and prolonged shelf life.

Acknowledgement

This work was financially supported by the Ministry of Education, Science and Technological Development, Republic of Serbia, Grant no. 172049.

References

[1] R.E. Mitchel, I.M. Chaiken, E.L. Smith, The complete amino acid sequence of papain. Additions and corrections, J. Biol. Chem. 245 (1970) 3485-3492.

[2] I.G. Kamphuis, K.H. Kalk, M.B.A. Swarte, J. Drenth, Structure of papain refined at 1.65 Å resolution, J. Mol. Biol. 179 (1984) 233-256.

[3] J. Weiss, M. Gibis, V. Schuh, H. Salminen, Advances in ingredient and processing systems for meat and meat products, Meat Sci. 86 (2010) 196-213.

[4] M.C. Lopes, R.C. Mascarini, B.M.C.G. da Silva, F.M. Flório, R.T. Basting, Effect of a Papain-based Gel for Chemomechanical Caries Removal on Dentin Shear Bond Strength, J. Dent. Child. 74 (2007) 93-97.

[5] R. Flanagan, A. Jones, Fab Antibody Fragments, Drug Safety, 27 (2004) 1115-1133.

[6] O. Kaiser, P. Aliuos, K. Wissel, T. Lenarz, D. Werner, G. Reuter, A. Kral, A. Warnecke, Dissociated Neurons and Glial Cells Derived from Rat Inferior Colliculi after Digestion with Papain, PLoS ONE, 8 (2013) e80490.

[7] Y.-C. Sim, S.-G. Lee, D.-C. Lee, B.-Y. Kang, K.-M. Park, J.-Y. Lee, M.-S. Kim, I.-S. Chang, J.-S. Rhee, Stabilization of papain and lysozyme for application to cosmetic products, Biotechnol. Lett. 22 (2000) 137-140.

[8] S.S. Khaparde, R.S. Singhal, Chemically modified papain for applications in detergent formulations, Bioresource Technol. 78 (2001) 1-4.

[9] H.A. Sathish, P.R. Kumar, V. Prakash, Mechanism of solvent induced thermal stabilization of papain, Int. J. Biol. Macromol. 41 (2007) 383-390.

[10] P.L. Privalov, Cold Denaturation of Protein, Crit. Rev. Biochem. Mol. Biol. 25 (1990) 281-306.

[11] S. Kunugi, N. Tanaka, Cold denaturation of proteins under high pressure, BBA - Protein Struct. M. 1595 (2002) 329-344.

[12] M. Davidovic, C. Mattea, J. Qvist, B. Halle, Protein Cold Denaturation as Seen From the Solvent, J. Am. Chem. Soc. 131 (2008) 1025-1036.

[13] F. Meersman, K. Heremans, High pressure induces the formation of aggregation-prone states of proteins under reducing conditions, Biophys. Chem. 104 (2003) 297-304.

[14] A. Tantos, P. Friedrich, P. Tompa, Cold stability of intrinsically disordered proteins, FEBS Lett. 583 (2009) 465-469.

[15] B.S. Bhatnagar, R.H. Bogner, M.J. Pikal, Protein Stability During Freezing: Separation of Stresses and Mechanisms of Protein Stabilization, Pharm. Dev. Technol. 12 (2007) 505-523.

[16] S. Singh, P. Kolhe, A. Mehta, S. Chico, A. Lary, M. Huang, Frozen State Storage Instability of a Monoclonal Antibody: Aggregation as a Consequence of Trehalose Crystallization and Protein Unfolding, Pharm. Res. 28 (2011) 873-885.

[17] M.M. Bradford, A rapid and sensitive method for the quantitation of microgram quantities of protein utilizing the principle of protein-dye binding, Anal. Biochem. 72 (1976) 248-254.

[18] U.K. Laemmli, Cleavage of Structural Proteins during the Assembly of the Head of Bacteriophage T4, Nature, 227 (1970) 680-685.

[19] R. Felicioli, B. Garzelli, L. Vaccari, D. Melfi, E. Balestreri, Activity staining of protein inhibitors of proteases on gelatin-containing polyacrylamide gel electrophoresis, Anal. Biochem. 244 (1997) 176-179.

[20] R. Hatley, F. Franks, The effect of aqueous methanol cryosolvents on the heat- and cold-induced denaturation of lactate dehydrogenase, Eur. J. Biochem. 184 (1989) 237-240.

[21] R. Yousefi, M. Imani, S.K. Ardestani, A.A. Saboury, N. Gheibi, B. Ranjbar, Human Calprotectin: Effect of Calcium and Zinc on its Secondary and Tertiary Structures, and Role of pH in its Thermal Stability, Acta Bioch. Bioph. Sin. 39 (2007) 795-802.

[22] B. Raskovic, O. Bozovic, R. Prodanovic, V. Niketic, N. Polovic, Identification, purification and characterization of a novel collagenolytic serine protease from fig (Ficus carica var. Brown Turkey) latex, J. Biosci. Bioeng. 118 (2014) 622-627.

[23] Z. Zhang, Z. He, G. Guan, Thermal stability and thermodynamic analysis of native and methoxypolyethylene glycol modified trypsin, Biotechnol. Tech. 13 (1999) 781-786.

[24] E. Goormaghtigh, V. Cabiaux, J.-M. Ruysschaert, Secondary structure and dosage of soluble and membrane proteins by attenuated total reflection Fourier-transform infrared spectroscopy on hydrated films, Eur. J. Biochem. 193 (1990) 409-420.

[25] G. Vedantham, H.G. Sparks, S. Sane, S. Tzannis, T. Przybycien, A Holistic Approach for Protein Secondary Structure Estimation from Infrared Spectra in H_2O Solutions, Anal. Biochem. 285 (2000) 33–49

[26] K. Goossens, J Haelewyn, F Meersman, M. de Ley, and K. Heremans, Pressure- and temperature-induced unfolding and aggregation of recombinant human interferon-γ: a Fourier transform infrared spectroscopy study, Biochem. J. 370 (2003) 529-535.

[27] A. Ismail, H. Mantsch, P. Wong, Aggregation of chymotrypsinogen: portrait by infrared spectroscopy, Biochim. Biophys. Acta 1121 (1992) 183-188.

[28] G.R. Grimsley, C.N. Pace, Spectrophotometric Determination of Protein Concentration, Current Protocols in Protein Science, John Wiley & Sons, Inc.2001.

[29] M. Manning, W. Colon, Structural basis of protein kinetic stability: resistance to sodium dodecyl sulfate suggests a central role for rigidity and a bias toward beta-sheet structure, Biochemistry, 43 (2004) 11248-11254.

[30] J. Yadav, V. Prakash, Thermal stability of α-amylase in aqueous cosolvent systems, J. Biosci. 34 (2009) 377-387.

[31] J.W. Donovan, Changes in Ultraviolet Absorption Produced by Alteration of Protein Conformation, J. Biol. Chem. 244 (1969) 1961-1967.

[32] P.F. Liu, L.V. Avramova, C. Park, Revisiting absorbance at 230 nm as a protein unfolding probe, Anal. Biochem. 389 (2009) 165-170.

[33] B. Wiederanders, The function of propeptide domains of cysteine proteinases, Adv. Exp. Med. Biol. 477 (2000) 261-270.

[34] J. Kong, S. Yu, Fourier Transform Infrared Spectroscopic Analysis of Protein Secondary Structures, Acta Bioch. Bioph. Sin. 39 (2007) 549-559.

[35] F. Meersman, L. Smeller, K. Heremans, Comparative Fourier Transform Infrared Spectroscopy Study of Cold-, Pressure-, and Heat-Induced Unfolding and Aggregation of Myoglobin, Biophys. J. 82 (2002) 2635-2644.

[36] C.L. Dias, T. Ala-Nissila, J. Wong-ekkabut, I. Vattulainen, M. Grant, M. Karttunen, The hydrophobic effect and its role in cold denaturation, Cryobiology, 60 (2010) 91-99.

[37] K. Matsuo, Y. Sakurada, S.-i. Tate, H. Namatame, M. Taniguchi, K. Gekko, Secondary-structure analysis of alcohol-denatured proteins by vacuum-ultraviolet circular dichroism spectroscopy, Proteins Struct. Funct. Bioinf. 80 (2012) 281-293.

[38] Y. Cordeiro, J. Kraineva, M.C. Suarez, A.G. Tempesta, J.W. Kelly, J.L. Silva, R. Winter, D. Foguel, Fourier Transform Infrared Spectroscopy Provides a Fingerprint for the Tetramer and for the Aggregates of Transthyretin, Biophys. J. 91 (2006) 957-967.

[39] C.L. Dias, Unifying Microscopic Mechanism for Pressure and Cold Denaturations of Proteins, Phys. Rev. Lett. 109 (2012) 048104.

[40] C.L. Dias, M. Karttunen, H.S. Chan, Hydrophobic interactions in the formation of secondary structures in small peptides, Phys. Rev. E, 84 (2011) 041931.

[41] Z. Su, C.L. Dias, Driving β-Strands into Fibrils, J. Phys. Chem. B, 118 (2014) 10830-10836.

[42] E. Gabellieri, G.B. Strambini, Perturbation of Protein Tertiary Structure in Frozen Solutions Revealed by 1-Anilino-8-Naphthalene Sulfonate Fluorescence, Biophys. J. 85 (2003) 3214-3220.

Figure legends

Figure 1. A) Chromatographic separation of papain on Thiol-Sepharose column. Column was equilibrated with 100 mM Tris buffer pH 8.0 containing 100 mM NaCl and 1 mM EDTA (Buffer A) followed by elution with the same buffer containing 10 mM cysteine (Buffer B). Chromatography was run with a flow rate of 0.8 mL/min. B) SDS-PAGE analysis and activity staining towards gelatin of each fraction collected during papain purification: 1 – starting commercial papain extract, 2 – acetone precipitate, 3 - thiol-Sepharose chromatography bound protein and M – molecular weight markers; C) Peptide mass fingerprint of the isolated papain, identified peptides are bolded and underlined.

Figure 2. A) UV absorption spectra from 255 nm to 300 nm of native papain (black line) and denatured papain (grey line); B) Differential UV absorption spectrum; C) Thermal denaturation curve of papain incubated at lowered and elevated temperatures. For creating the curve A_{267} was monitored as a function of temperature over the appropriate temperature range (5-99 °C). The heating rate was 0.5 °C min^{-1}. The percentage of native structure was calculated as the percentage of maximal change of the extinction coefficient ($\Delta\varepsilon$).

Figure 3. Activity of papain during six freeze–thaw cycles. Activity of starting papain sample (C) is considered as 100%, and the measured activity after each freeze–thaw cycle (1X – 6X) is expressed as a percent of starting activity. Data represent the mean of three separate experiments.

Figure 4. A) Autoproteolysis of papain during 6 freeze-thaw cycles. The absorbance of each sample is shown as a percentage of the initial absorbance. B) RP-HPLC of of native (black line) and cold stored papain (grey line).

Fig. 5. Second derivative FT-IR spectrum of: A) native papain; B) thermally treated papain and C) cold stored papain.

Fig. 6. A) The original and curve-fitted FT-IR spectrum of: A) native papain; B) thermally treated papain and C) cold stored papain.

Figure 7. Size exclusion chromatograpy analysis of native (black line) and cold stored papain (grey line). BD, BSA, CA, CC and A - gel filtration molecular weight standards (blue dextran 2,000 kDa, bovine serum albumin 67 kDa, carbonic anhydrase 29 kDa, cytochrome c 14 kDa and aprotinin 6.5 kDa, respectively).

Supplementary Figure 1. DSC thermogram of papain in 50 mM Tris buffer pH 8.0.

A)

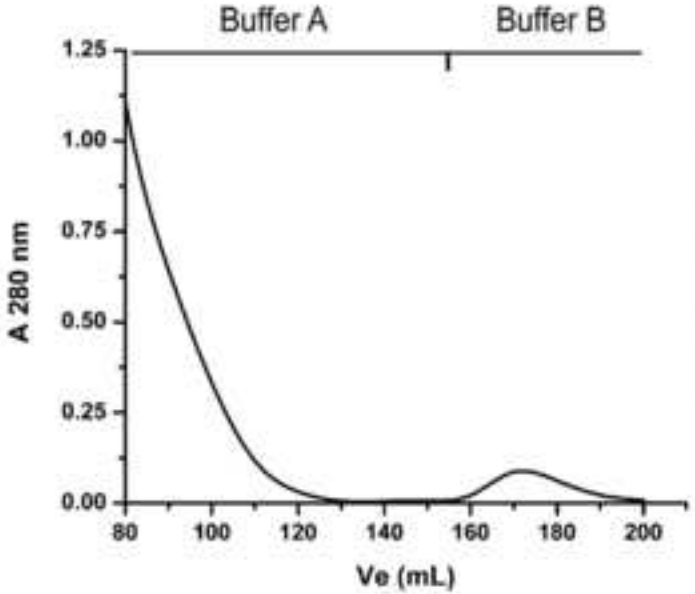

B)

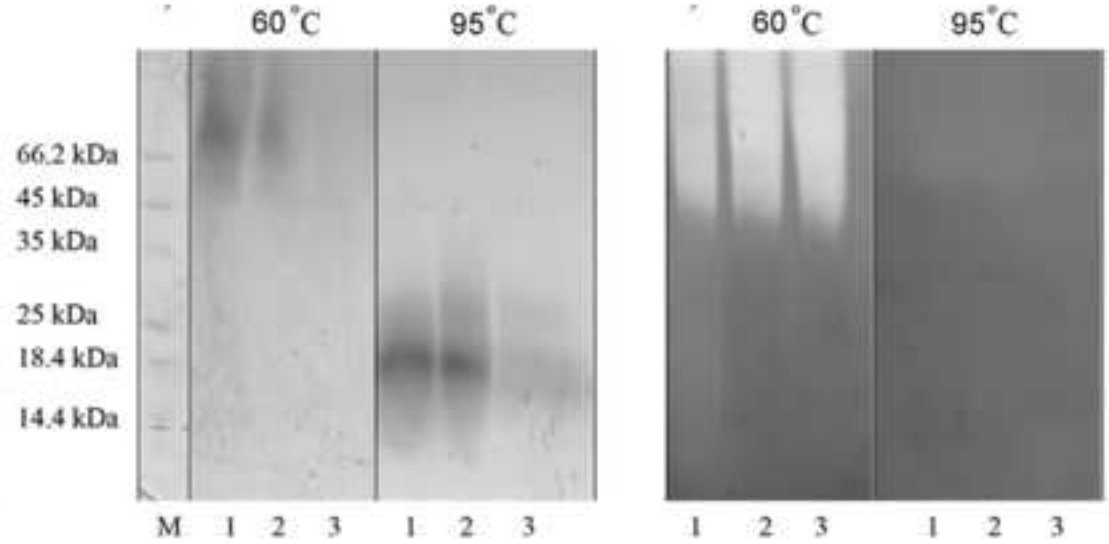

C)

1 IPEYVDWR**QK GAVTPVK**NQG SCGSCWAFSA VVTIEGIIKI RTGNLNEYSE

51 QELLDCDRRS YGCNGGYPWS ALQLVAQYGI HYR**NTYPYEG VQRYCRSREK**

101 **GPYAAKTDGV R**QVQPYNEGA LLYSIANQPV SVVLEAAGK**D FQLYR**GGIFV

151 GPCGNKVDHA VAAVGYGPNY ILIKNSWGTG WGENGYIR**IK R**GTGNSYGVC

201 GLYTSSFYPV KN

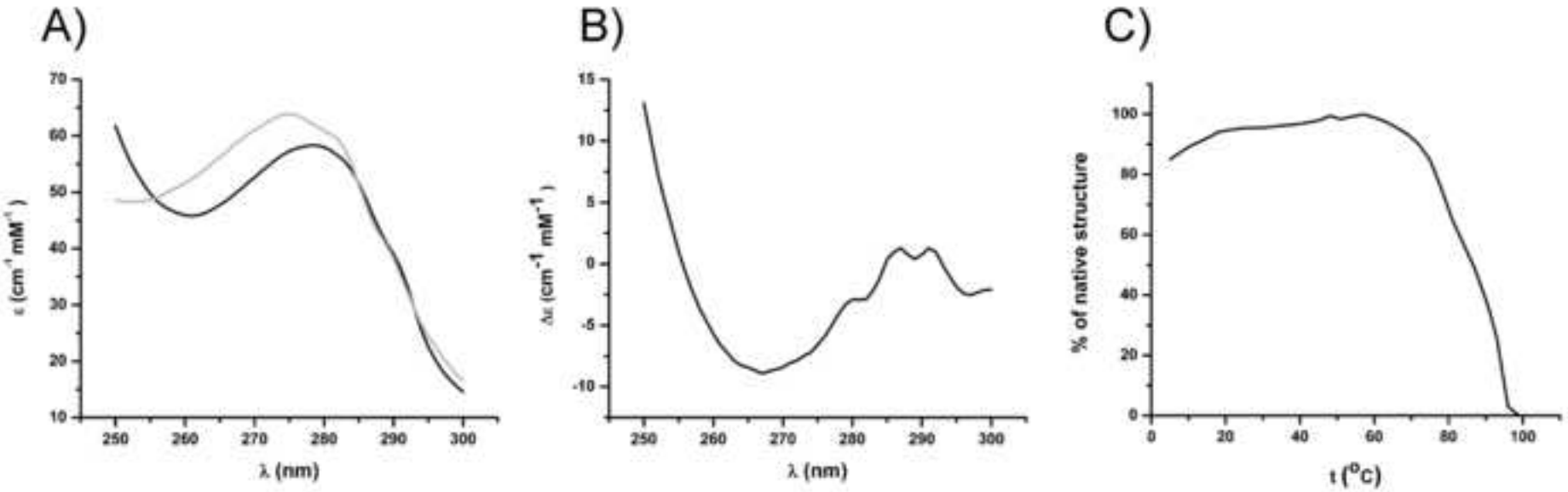

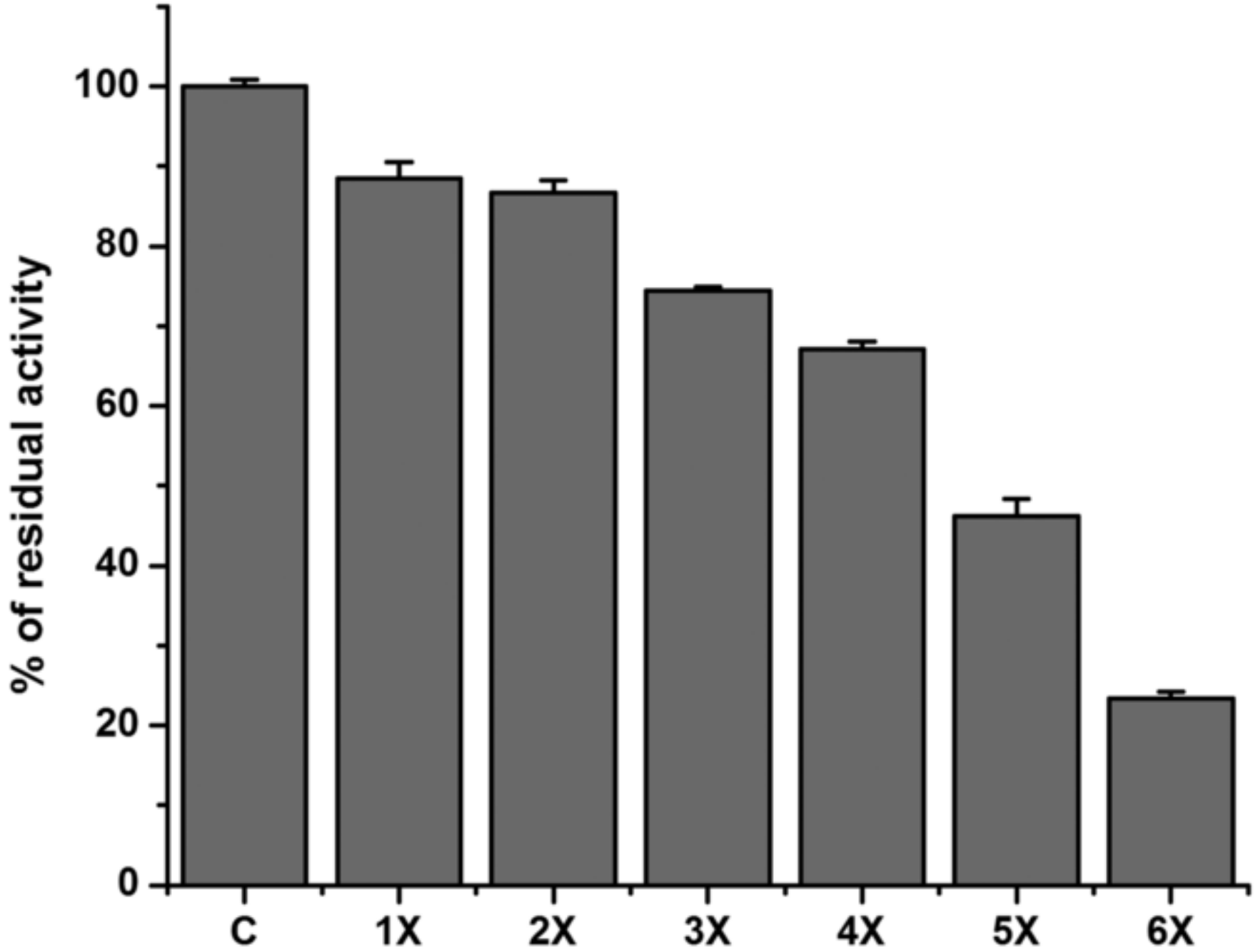

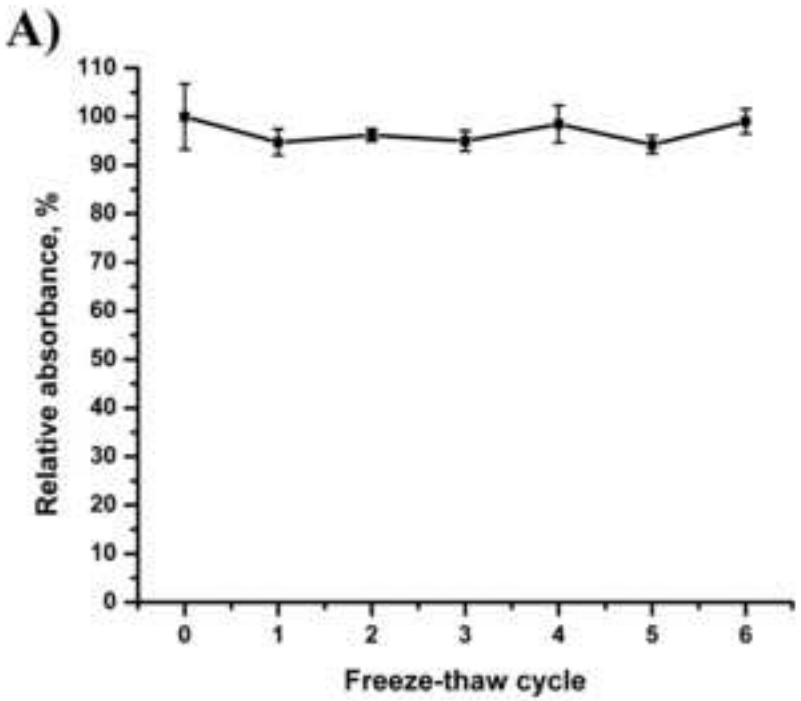

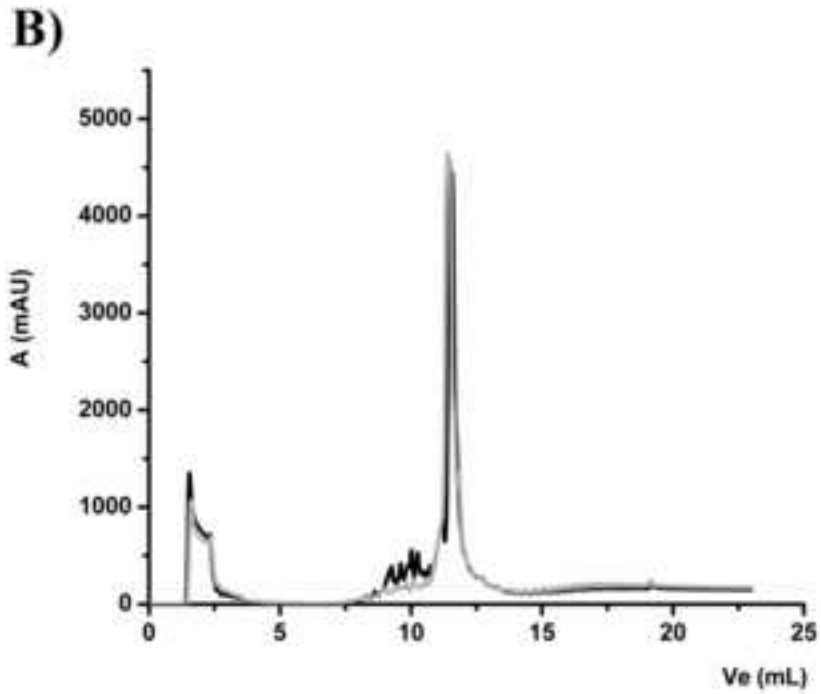

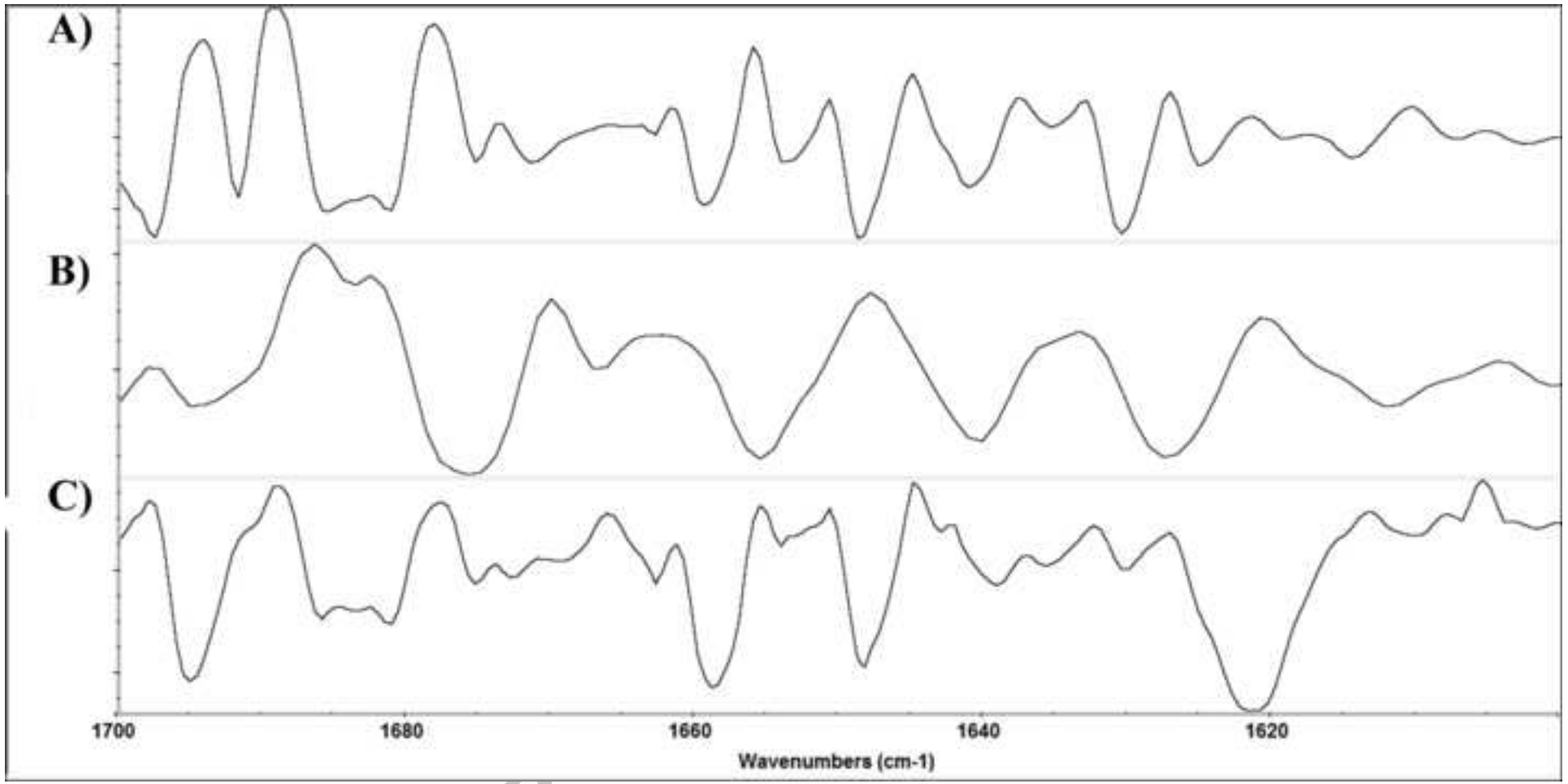

A)

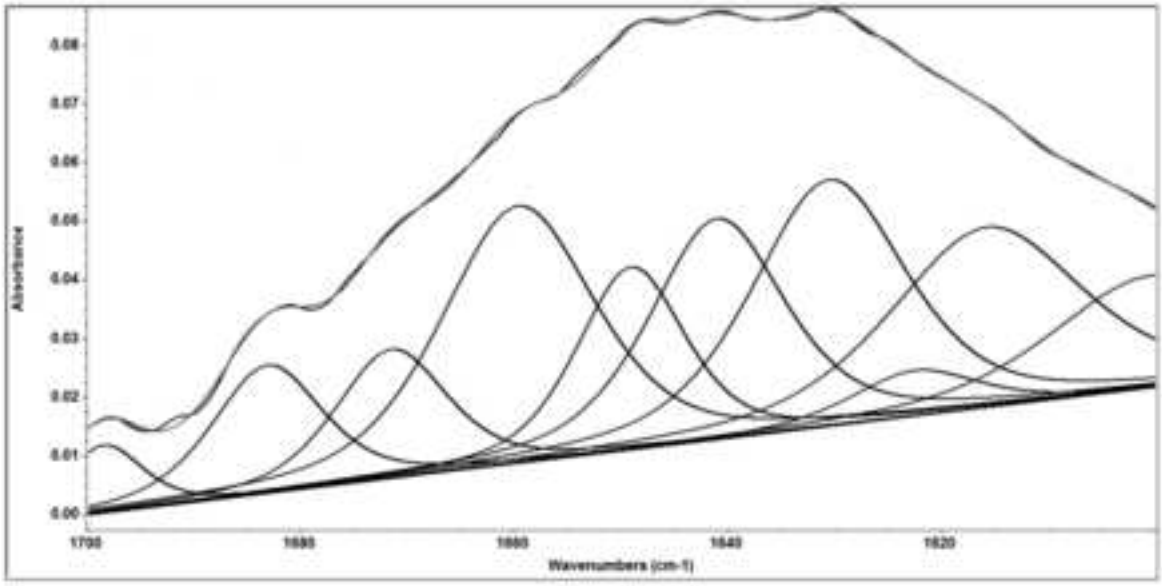

B)

C)

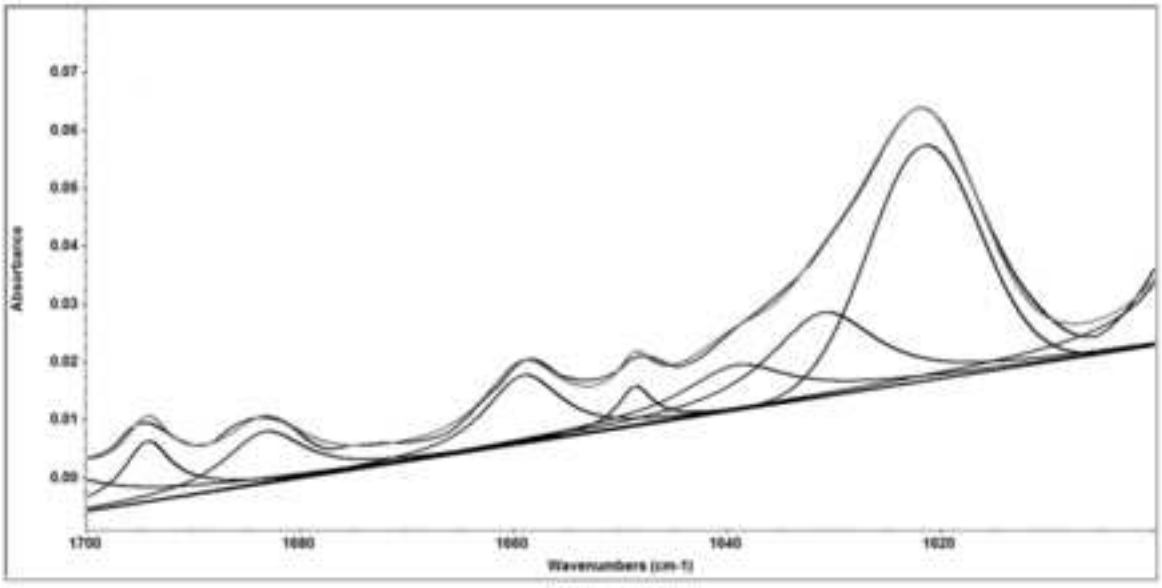

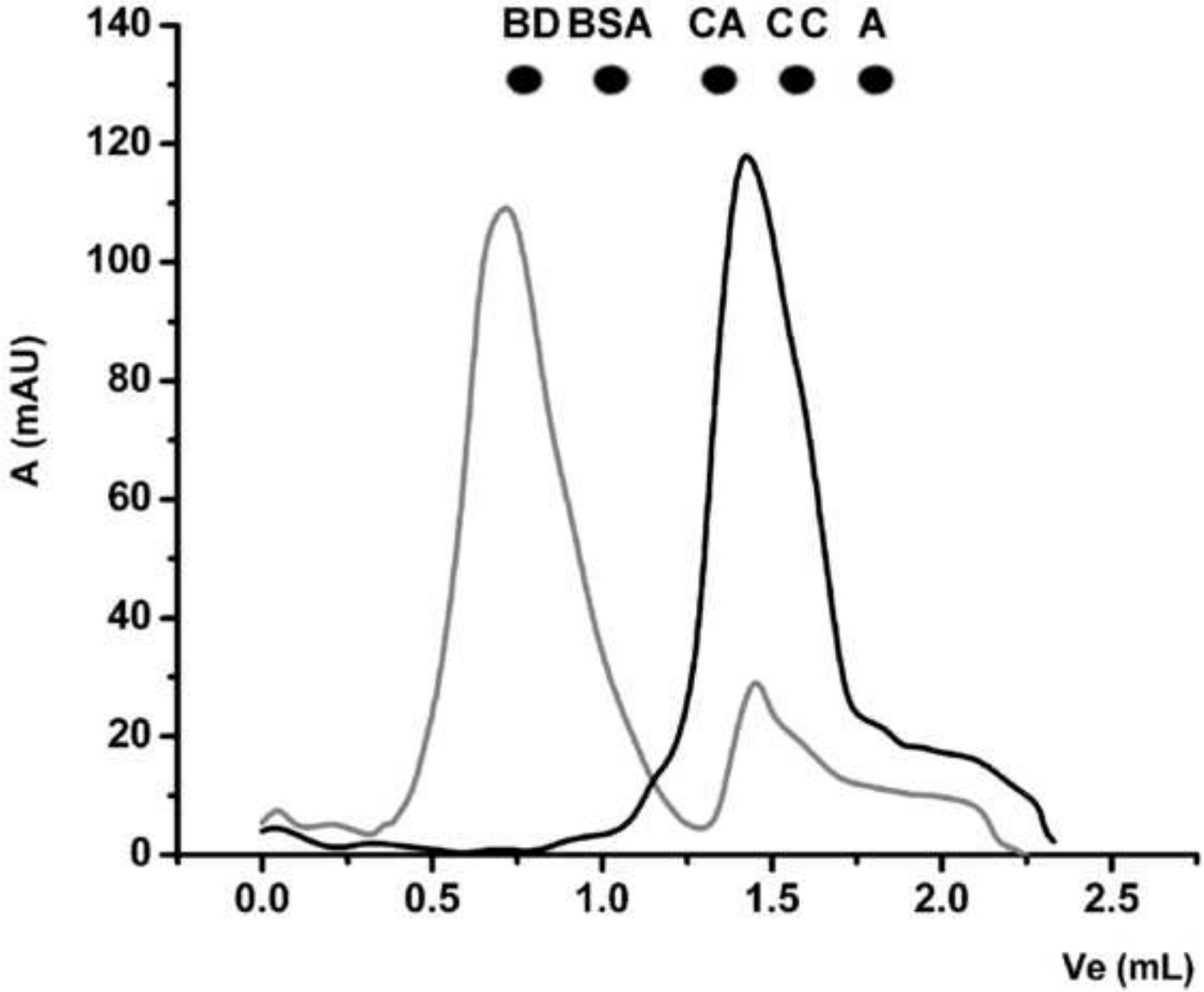

Table 1. Purification of papain.

	Activity (U/mL)	**Protein concentration, (mg/mL)**	**Specific activity, (U/mg)**	**Purification degree**
Crude extract	83.3 ± 0.5	15.3 ± 0.2	1.13	1
Acetone precipitation	73 ± 1	13.6 ± 0.5	1.12	0.99
Covalent chromatography	3.9 ± 0.1	0.091 ± 0.002	9.0	7.9

Table 2. The Gibbs free energy change (ΔG^o) of thermal stability of papain. ΔG^o was calculated from the equation $\Delta G^o = - RTlnK$ where R is the universal gas constant and T is the absolute temperature.

	ΔG^o_{278} (kJ/mol)	**ΔG^o_{298} (kJ/mol)**	**ΔG^o_{321} (kJ/mol)**	**ΔG^o_{333} (kJ/mol)**
Papain	3.2 ± 0.1	7.5 ± 0.3	13.9 ± 0.3	12.5 ± 0.4

Table 3. Assignments and relative band areas of Amide I components of native, thermally treated and cold stored papain. Relative band areas were determined by curve-fitting analysis. Inter – intermolecular; Intra – intramolecular β-sheet.

Native papain		Thermally treated papain		Cold stored papain		
ν (cm^{-1})	Area (%)	ν (cm^{-1})	Area (%)	ν (cm^{-1})	Area (%)	Assignment
1623	3.6	1618	9.1	1621	38.7	Inter/Intraβ [24-27]
1630	22.8	1628	27.2	1629	19.2	Inter β-sheet [24]
1641	19.8	1641	9.7	1639	11.7	Random coil [24]
1648	10.8	-	-	1648	3.4	α-helix [24]
1659	21.3	1653	20.6	1659	10.7	α-helix [24]
1672	9.9	1974	8.2	-	-	Unordered helix [25]
1683	8.5	1663	13.0	1683	8.8	Turn [24]
1697	3.3	1698	12.2	1695	7.5	Inter/Intraβ [24-26]

Table 4. Fitted values for the secondary structures present in the native, thermally treated and cold denatured papain determined by ATR FT-IR spectroscopy and secondary structure contents calculated from X-ray analysis.

Papain sample	**Secondary structure content (%)**					
	β-sheet	α-helix	Unordered structures	Turn	Inter/Intramolecular β-sheet	RMS error
Native	22.8	32.1	29.7	8.5	6.2	3.5
Thermally treated	27.2	20.6	17.9	13.0	21.3	0.1
Cold stored	19.2	11.7	14.1	8.8	46.2	1.4
X-ray	25	26	42	7	-	-

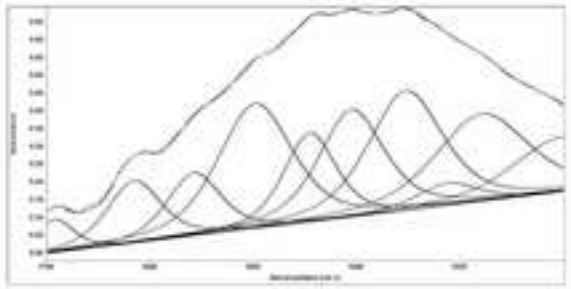

PAPAIN

Cold storage

- Aggregation
- Denaturation
- Inactivation

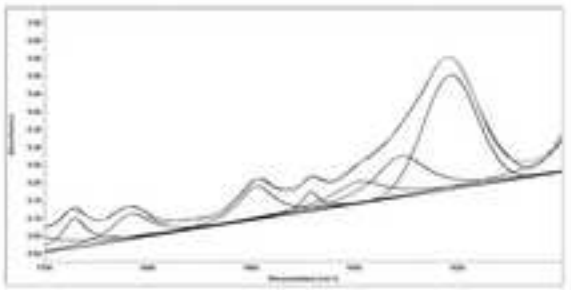

Highlights

- Papain was the most stabile from 45 to 60ºC with ΔG^{o}_{321} 13.9 kJ/mol and Tm value 84ºC
- Cold storage of papain gave an increase of 40% of intermolecular β-sheet content
- Six freeze-thaw cycles induced 75% activity loss due to denaturation and aggregation
- Autoproteolysis of papain did not cause significant loss of the protein activity